The Journal of Experimental Biology 211, 1882-1892
Published by The Company of Biologists 2008
doi:10.1242/jeb.014407

Motor unit recruitment patterns 1: responses to changes in locomotor velocity and incline

Emma F. Hodson-Tole[1,*] and James M. Wakeling[2]

[1]The Structure and Motion Laboratory, The Royal Veterinary College, Hawkshead Lane, North Mymms, Hatfield, Herts, AL9 7TA, UK and [2]School of Kinesiology, Simon Fraser University, Burnaby, BC, V5A 1S6, Canada

*Author for correspondence at present address: The School of Applied Physiology, Georgia Institute of Technology, Atlanta, GA 30332, USA (e-mail: etole@gatech.edu)

Accepted 17 March 2008

SUMMARY

Mammalian skeletal muscles are composed of a mixture of motor unit types, which contribute a range of mechanical and physiological properties to the muscle. For a muscle to effectively contribute to smooth, co-ordinated movement it must activate an appropriate number and combination of motor units to generate the required force over a suitable time period. Much evidence exists indicating that motor units are activated in an orderly fashion, from the slowest through to the fastest. A growing body of evidence, however, indicates that such a recruitment strategy does not always hold true. Here we investigate how motor unit recruitment patterns were influenced by changes in locomotor velocity and incline. Kinematics data and myoelectric signals were collected from three rat ankle extensor muscles during running on a treadmill at nine velocity and incline combinations. Wavelet and principal component analysis were used to simultaneously decompose the signals into time and frequency space. The relative frequency components of the signals were quantified during 20 time windows of a stride from each locomotor condition. Differences in signal frequency components existed between muscles and locomotor conditions. Faster locomotor velocities led to a relative increase in high frequency components, whereas greater inclines led to a relative increase in the low frequency components. These data were interpreted as representing changes in motor unit recruitment patterns in response to changes in the locomotor demand. Motor units were not always recruited in an orderly manner, indicating that recruitment is a multi-factorial phenomenon that is not yet fully understood.

Key words: electromyography, size principle, wavelet analysis, principal component analysis.

INTRODUCTION

The basic functional unit of the neuromuscular system is the motor unit, which is defined as being an α-motoneuron and all the muscle fibres that it innervates (Sherrington, 1929). The metabolic and mechanical properties of motor units have been extensively researched and a number of classification systems have been developed based on physiology (Burke et al., 1973), metabolism (Peter et al., 1972) and myosin heavy chain profile (Schiaffino et al., 1989). Most tetrapod muscles contain a mixture of muscle fibre types whose recruitment and interaction facilitates effective movement over a wide range of speeds and loads. Through studying stretch reflexes in decerebrate cats it has been found that as activation stimulus increases successively larger motor units are recruited in an orderly fashion termed the 'size principle' (Henneman et al., 1965a; Henneman et al., 1965b). Motor unit size has been shown to vary both within and between muscles with a trend for smaller units to be composed of slower twitch muscle fibres and larger motor units to be composed of faster twitch fibres (McPhedran et al., 1965a; McPhedran et al., 1965b). In addition, smaller motor units have smaller diameter nerve axons, which result in slower action potential conduction velocities along them (Bawa et al., 1984). The size principle therefore predicts that, based on both contractile properties and action potential conduction velocities, faster motor units will be recruited after slower motor units have been activated and will be the first motor units to be derecruited.

To date, methods to study *in vivo* patterns of motor unit recruitment have been limited. A myoelectric signal is composed of an interference pattern of the action potentials of all active motor units within the vicinity of the detecting electrode(s). The action potentials from different types of motor unit differ in shape and conduction velocity (Albuquerque and Thesleff, 1968; Luff and Atwood, 1972), and hence information on the type of motor units active are contained within the frequency component of the myoelectric signal, with faster motor units generating higher frequency spectra (Kupa et al., 1995; Wakeling and Syme, 2002). The mean and/or median frequency values of the power spectra of the myoelectric signals are influenced by a number of physiological properties including muscle fascicle length (Doud and Walsh, 1995), fatigue (Brody et al., 1991) and motor unit recruitment (Wakeling and Rozitis, 2004). Mean frequencies, however, cannot uniquely identify motor unit recruitment as an increase in the mean frequency may occur due to increased activity in faster motor units, or may result from a reduction in activity in slower motor units. It is not possible to distinguish between the two explanations and therefore this technique does not provide as sensitive a method of quantifying motor unit recruitment as may be desirable in some circumstances. More recently von Tscharner (von Tscharner, 2000) has developed a set of myoelectric-specific wavelets, which enable changes in the frequency content of the signal to be identified in more detail. These wavelet transform techniques have been applied in a number of studies of man (Mundermann et al., 2006; von Tscharner, 2002;

Von Tscharner and Goepfert, 2006; Wakeling et al., 2001a; Wakeling and Rozitis, 2004; Wakeling et al., 2006; Wakeling et al., 2001b), and to a lesser extent to data collected from a number of animal models (Hodson-Tole and Wakeling, 2007; Wakeling et al., 2002; Wakeling and Syme, 2002). These studies have indicated that there is a surprising amount of variation in patterns of motor unit recruitment during locomotion and have highlighted the need to study this phenomenon in more detail.

In this and a companion paper (Hodson-Tole and Wakeling, 2008) we aim to: (1) describe changes in motor unit recruitment patterns in response to changes in locomotor velocity and incline; (2) determine what underlying factors may influence the recorded motor unit recruitment patterns (Hodson-Tole and Wakeling, 2008). In this first study we therefore aim to quantify patterns of motor unit recruitment within the three ankle extensor muscles of the rat (*Rattus norvegicus*) during treadmill locomotion at different velocities and inclines. The rat was chosen as a suitable model for these studies because it is easily trained to perform a range of tasks and it is possible to take detailed measurements of the rat system using a combination of sonomicrometry and electromyography (Gillis and Biewener, 2001). There is also a wide range of information available on the contractile properties of rat muscles (Close, 1964; Close and Luff, 1974; Schiaffino and Reggiani, 1996). The soleus, plantaris and medial gastrocnemius muscles were studied as these contain predominantly slow, fast and a mixed population of muscle fibre types, respectively (Armstrong and Phelps, 1984). Comparing synergistic muscles with such differences in fibre type proportions, and hence mechanical properties, facilitated analysis of recruitment strategies within distinctly different fibre populations during different locomotor tasks. It was hypothesised that increasing locomotor velocity and incline would lead to an increase in myoelectric intensity in each muscle. In addition, it was hypothesised that increased locomotor velocity would lead to an increase in the high frequency myoelectric signal component from each muscle. An increase in locomotor incline was hypothesised to lead to an increase in the low frequency component of the myoelectric signal from each muscle, as we predicted the recruitment of slower motor units to provide the additional forces required for the mechanical work of overcoming gravity.

MATERIALS AND METHODS

Subjects

Myoelectric data were collected from the soleus, plantaris and medial gastrocnemius muscles of the right hind limb of 12 female Sprague Dawley rats [251.82±21.04 g (mean mass ± s.d.), approximate age 5–6 months; Table 1). All rats had undergone a 5 week training programme to habituate them to run on a custom-made motorised treadmill at nine velocity (20–50 cm s^{-1}) and incline (0–25°) combinations. Prior to data collection, all rats were able to maintain a steady position on the treadmill belt for at least 60 s during each locomotor condition. Subjects were housed in pairs in a temperature controlled room (20°C) with a 12 h:12 h light:dark cycle. Standard rat chow and water were available *ad libitum*. All procedures were carried out in accordance with current UK Home Office regulations.

Surgical procedures

The information presented here provides a detailed description of the complete surgical procedures used to implant myoelectric and sonomicrometric transducers. For the purposes of this study only myoelectric data have been analysed and presented. Sonomicrometric data are presented in the companion study (Hodson-Tole and Wakeling, 2008), where details of subject numbers and analysis techniques are presented.

Table 1. Details of myoelectric data collected from each subject

	Muscle		
Subject	M. gastrocnemius	Plantaris	Soleus
1	X	X	
2	I	X	
3	X		X
4	X		X
5	I		X
6	X		I
7		I	X
8		X	X
9		I	X
10		X	I
11	X	X	
12	X	X	

X indicates that data were collected, analysed and presented as part of this study; I indicates that transducers were implanted but data were not assessed as part of this study.

Halothane gas (4.0% induction; 1.75–2.0% maintenance) was used to anaesthetise subjects following a subcutaneous injection of atropine (0.01 mg kg^{-1}). The right hind limb and an area of the back in the region of the shoulder blades was shaved and scrubbed with 4% chlorhexidine gluconate solution (E-Z Scrub, Becton, Dickinson and Co., Franklin Lakes, NJ, USA) and painted with a povidone-iodine solution. An ocular solution (Lacri-Lube®, Allergan Ltd, Marlow, UK) was applied to each eye. An initial incision was made along the lateral aspect of the limb, approximately parallel to the tibia and over the fascia of the biceps femoris. A second incision was made caudal to the scapulae and a subcutaneous tunnel created between the two incisions. Before the removal of the tunnelling device the wires from the transducers to be implanted were fed through it, so the transducers were present at the muscle site and excess wire externalised in the region of the scapulae.

Owing to the small size of the muscles being investigated it was not possible to simultaneously place myoelectric and sonomicrometric transducers into each muscle. Therefore, in each subject, offset twist-hook bipolar silver-wire electrodes (0.1 mm diameter, California Fine Wire Inc., Grover Beach, CA, USA), with tips bared of 0.5 mm of insulation were inserted into two of the muscles of interest using fine-tipped forceps. The electrode tips were approximately 2 mm apart and implanted at a depth of approximately 3 mm. In the soleus and plantaris muscles, electrodes were placed in the mid-belly of the muscle, whereas in the medial gastrocnemius muscle, electrodes were placed in the medio-caudal region, corresponding to an area identified as having a mixture of predominantly MHC type IIB fibres (Armstrong and Phelps, 1984). In the third muscle, not containing fine-wire electrodes, two sonomicrometry crystals (1.0 mm, plus 38-gauge stainless steel lead wires; Sonometrics Corps., London, ON, Canada) were inserted into pockets created in the proximal and distal ends of the muscle using fine-tipped forceps. Once each crystal was in position the pocket was sutured shut using 5-0 prolene to secure the crystal in place. Slack wire from the fine-wire electrodes and the crystals were fed under the skin into the area surrounding the hip, ensuring that the animal had the full range of movement of the limb and was not restricted by the presence of the wires. Excess wire externalised in the region of the shoulder blades was placed into a small cotton pouch, which was secured under a small jacket fashioned for each

subject from elasticated bandage (Vetrap™, 3M United Kingdom PLC, Bracknell, UK). The jacket protected the wound and the wires and enabled the animals to be kept in their pairs during the recovery period. All subjects received post-operative analgesia (buprenorphine, 0.01 mg kg^{-1}, subcutaneously) during the 48 h recovery period. No animals showed any signs of post-operative infection (no antibiotics were administered) and normal behaviour was observed in all subjects prior to data collection.

Data collection

All data were collected in an electrically shielded room, 48 h post surgery. During each trial, kinematics data (100 frames per second) from the right hind limb were collected using two cameras (A602f, Basler, Ahrensberg, Germany), running off digital triggers and connected to the data collection computer *via* IEEE 1394 ports. Myoelectric signals (3200 Hz) were amplified (CP511 A.C. amplifier, Astro-Med, Inc., West Warwick, USA), bandpass filtered (30–1000 Hz) and collected through a 16-bit data acquisition card (PCI-6221, National Instruments Corps., Austin, TX, USA). Sonomicrometry signals (715 Hz) were collected using Sonometrics systems hardware (Sonometrics Corps.) and relayed to the data collection computer. All data were collected for periods of 30 s, having been synchronously triggered *via* the data acquisition card. Custom-written software (LabView 7.1, National Instruments Corps.) synchronised collection of myoelectric, sonomicrometric and video data streams. Each rat ran a three block randomised exercise programme incorporating nine speed and incline combinations (0° at 20, 30, 40 and 50 cm s^{-1}; 10° at 20, 30 and 40 cm s^{-1}; 20° at 20 cm s^{-1} and 25° at 20 cm s^{-1}). On completion of the trials animals were euthanased using intraperitoneal pentobarbitone and dissection carried out to confirm the location of the fine-wire electrodes and sonomicrometry crystals and determine muscle morphological characteristics.

Determination of muscle morphology

Following euthanasia the left hind limbs of six of the subjects (mass 258.37±12.57 g; mean ± s.d.) were skinned and the superficial muscle layers removed to reveal the ankle extensor muscles. Each limb was pinned to a corkboard with the sagittal plane joint angles set to those corresponding to a standing rat (hip 60°; knee 90°; ankle 90°), determined from previously recorded fluoroscopy images (not presented here). While the muscles were *in situ* total muscle tendon unit length, muscle belly length and external tendon length were measured. On removal of the muscles from the limb, muscle mass, less any external tendon, was recorded using digital weigh scales (PM480 Delta Range, Mettler-Toledo Ltd, Leicester, UK). At eight points, distributed along the length of the muscle belly, fascicle lengths were measured using the digital callipers (accurate within 0.15 mm; World Precision Instruments, Stevenage, UK). An incision was made into each muscle, parallel to the line of pull of the tendon, and pennation angle was determined in eight places along the incision. Muscle volume was calculated by dividing muscle mass by a standard vertebrate, skeletal muscle density of 1.06 g cm^{-3} (Mendez and Keys, 1960). Cross-sectional area (A_m) was determined as the quotient of muscle volume and mean fascicle length, and physiological cross-sectional area (A_{pm}) was determined as the product of A_m and the cosine of the pennation angle (η) (Powell et al., 1984).

Determination of temporal stride characteristics

Temporal stride characteristics were quantified using video data of the subjects' lateral aspect, collected from each trial. Customised software (LabView 8.0, National Instruments Corps.) was used to determine the frame numbers in which foot on and foot off occurred. Foot on was defined as the frame in which the right hind foot was first seen to be in contact with the treadmill belt. Foot off was defined as the last frame in which the right hind foot was seen to be in contact with the treadmill belt. A stride was defined as occurring between successive right hind footfalls. Stance phase was defined as occurring when the right hind foot was in contact with the treadmill belt, between successive foot on and foot off records. The swing phase was defined as occurring between successive foot off and foot on records. Temporal stride characteristics were determined for all strides when the rat was maintaining a steady position on the treadmill belt. A steady position was defined by eye, and was said to occur when the rat maintained its position within the running area defined by the perspex box surrounding it, i.e. did not accelerate forward or drift backward.

Analysis of myoelectric data

Myoelectric data from rats exercising at 40 cm s^{-1} on a level treadmill have previously been reported (Hodson-Tole and Wakeling, 2007). They are re-presented here to provide a complete overview of the changes in motor unit recruitment patterns that occur in response to changes in locomotor velocity and incline.

Wavelet transformation of the myoelectric signal

Analysis of the myoelectric data followed previously reported methods (Hodson-Tole and Wakeling, 2007). Briefly, the myoelectric signals were decomposed into time and frequency components using a filter bank of 20 non-linearly scaled wavelets indexed by $0 \leqslant k \leqslant 19$. The methods of von Tscharner (von Tscharner, 2000) were used to define each wavelet in terms of its frequency bandwidth, centre frequency (f_c) and time resolution. The raw signal was convoluted with each of the wavelets, with the intensity of the signal at each wavelet domain calculated at each time point from the magnitude and the first time-derivative of the square of the convoluted signal (von Tscharner, 2000). Power spectra, derived from Fourier transforms, revealed a quantity of low frequency noise (<100 Hz) to be present in the myoelectric signals collected. A large proportion of the noise was removed from the signal by removing wavelet domains $0 \leqslant k \leqslant 3$ from further analysis (Hodson-Tole and Wakeling, 2007). This method enabled 95% of the original signal to be preserved across the frequency band 69.92–1325.00 Hz. Slow motor units in the rat, recorded using fine-wire electrodes, have been shown to produce signals at 183.3±7.9 Hz (Wakeling and Syme, 2002), and we are therefore confident that signals from these motor units are present in the analysis presented. The wavelet transformed myoelectric signals from each of the muscles were partitioned into complete strides defined, using video data, by consecutive foot on times of the right hind limb (total number of strides analysed: soleus 4372; plantaris 3530; medial gastrocnemius 4385). The total intensity at a given time, i, was calculated by summing the intensities over all the included wavelets ($4 \leqslant k \leqslant 19$), so that i_k denotes the myoelectric intensity for any time point at wavelet domain k. The myoelectric intensity therefore provides a measure of the power within the signal at well-defined time intervals (Fig. 1). The instantaneous mean frequency (f_m) was calculated from:

$$f_m = \frac{\sum_k f_c(k) i_k}{\sum_k i_k}, \quad (1)$$

with f_c representing the centre frequency of each wavelet and the mean frequency calculated as the mean of the f_m values taken from

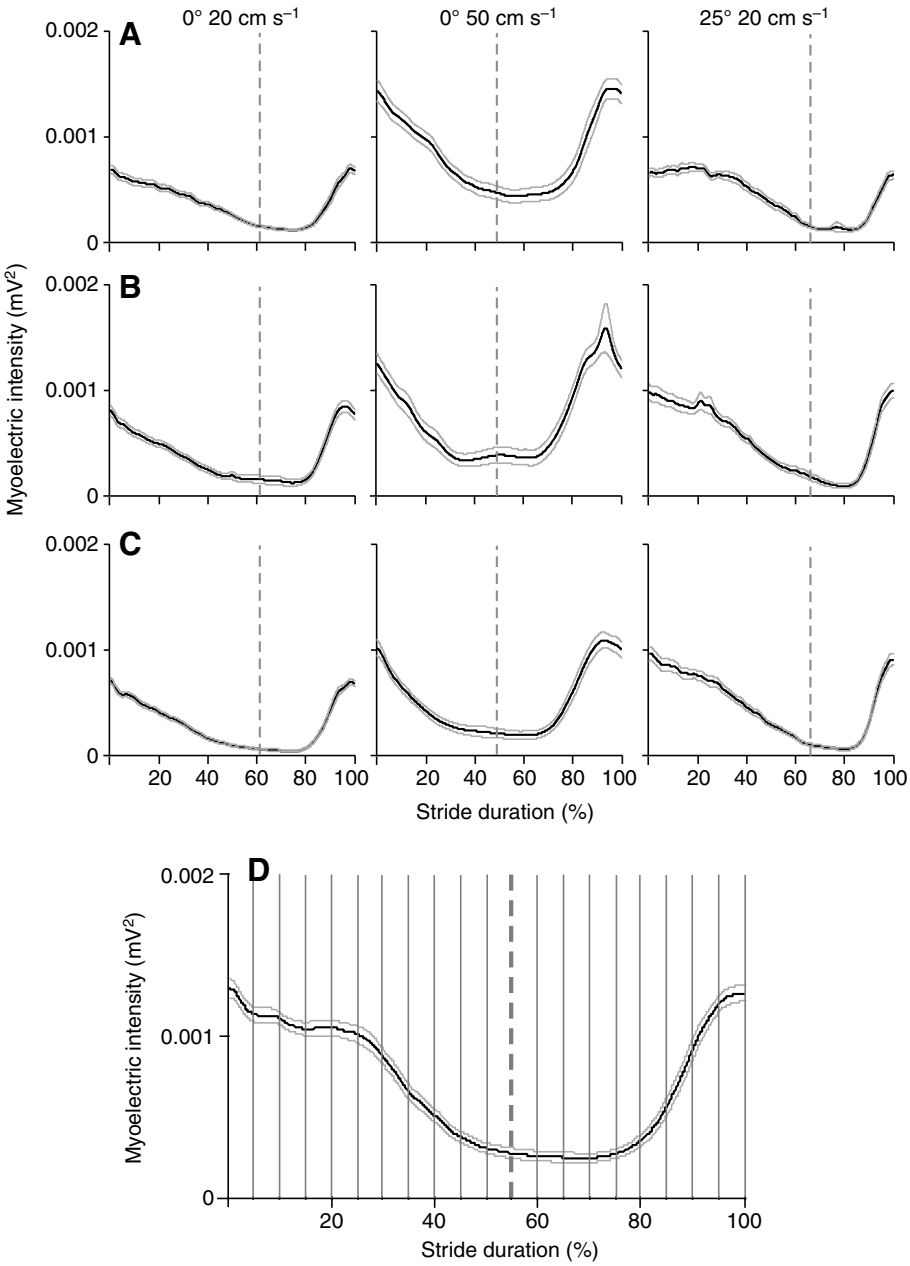

Fig. 1. Mean myoelectric intensity spectra for the plantaris (A), soleus (B) and medial gastrocnemius (C) muscle during three locomotor conditions (N=6 for each muscle). Data are shown as mean (black line) and s.e.m. (grey lines), with the division between stance and swing phase denoted by the broken, grey vertical line; 0% stride duration represents initial ground contact. Partitioning of the stride is represented in D, including data from the plantaris muscle (10° 40 cm s^{-1}). The division between stance and swing phase is shown by the broken, thick, vertical grey line.

whole strides. To determine changes in motor unit recruitment over the time course of a stride, data from each stride were partitioned into 20 equal time windows and mean values calculated for each time window, prior to the next step in the analysis (Fig. 1D).

Principal component analysis

Principal component (PC) analysis followed the techniques previously reported (Hodson-Tole and Wakeling, 2007). Briefly, the data sets were aligned into a $p\times N$ data matrix **A**, where p=16 wavelet domains and N=245 740 partitioned spectra included in the analysis (12 287 total number of strides×20 partitioned spectra). The principal components, eigenvector–eigenvalue pairs, were determined for the covariance matrix of matrix **A**. To ensure the analysis described the whole signal, and not just its variance, calculations were made on the total intensity values without prior subtraction of the mean (Wakeling and Rozitis, 2004). Over 94% of the original spectra were described by the first two principal components (PCI 89.64%; PCII 5.07%; PCIII 1.47%; PCIV 0.89%), which enabled the spectra to be expressed in fewer terms than the original wavelet transformation used (Wakeling and Rozitis, 2004).

The principal component weighting is given by the eigenvector, and can be displayed graphically as a function of the centre frequencies of the corresponding wavelets (Fig. 2A). The principal component loading score is given by the eigenvalue, and is a scalar value that describes the amount of each eigenvector in each measured spectrum. Each spectrum can be reconstructed by a linear combination of the principal component weightings and their loading scores. PCI loading scores have been shown to correlate with total myoelectric intensity and hence provide a good measure of myoelectric activity, whereas PCII loading scores relative to PCI loading scores provide a measure of the relative frequency content within the signal (Hodson-Tole and Wakeling, 2007; Wakeling, 2004). A quantitative measure of the contribution of high and low frequency content within the myoelectric signal is thus given by the

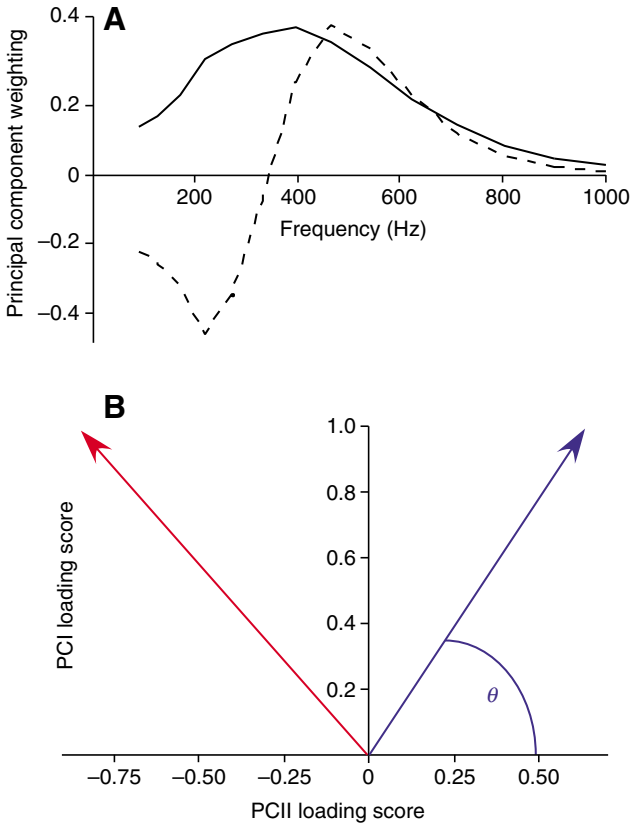

Fig. 2. Results of the principal component analysis. (A) The first two principal components (PCI, solid black line; PCII, broken black line) defined from the partitioned myoelectric spectra of all muscles under all conditions (N=245 740). (B) Vector representation of the spectra reconstructed from the PC weightings shown in A, with PCI –0.76 PCII (red) and PCI +0.54 PCII (blue), indicating the angle θ.

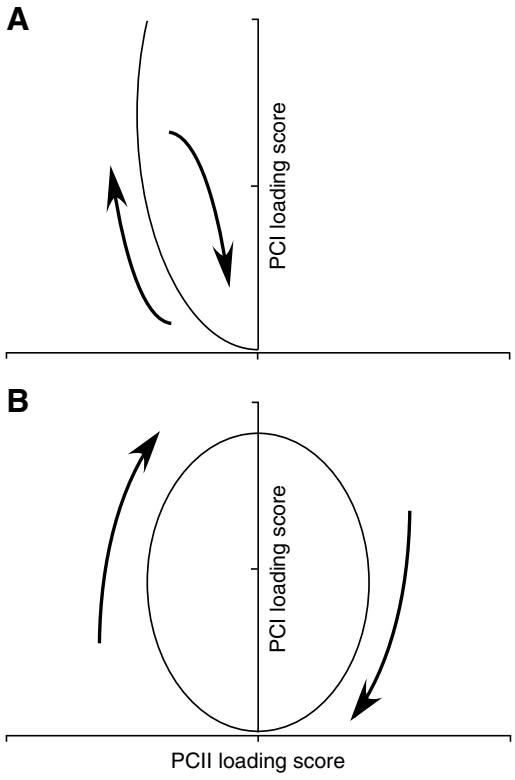

Fig. 3. PCI–PCII loading score vector plots representing the changes in θ that would be expected to occur if: (A) orderly recruitment of motor units occurred with slower motor units activated before and deactivated after faster motor units; (B) slower motor units were activated and deactivated in advance of activation and deactivation of faster motor units.

angle formed between the PCI and PCII loading scores (θ) (Hodson-Tole and Wakeling, 2007; Wakeling, 2004; Wakeling and Rozitis, 2004). Large angles of θ represent a relatively large low frequency signal component, whereas small angles of θ represent a relatively large high frequency signal component (Fig. 2B). In the present study θ was therefore used as a measure of myoelectric signal frequency content and hence patterns of motor unit recruitment. As the size principle predicts slower motor units are recruited before and derecruited after faster motor units and that a given level of muscle activity (represented by PCI loading scores) is achieved by activation of one combination of motor units (represented by θ), this pattern would be represented as a single line in the PCI–PCII loading score plane (Fig. 3A). If slower motor units were recruited before faster motor units and derecruited before faster motor units a clockwise loop in the PCI–PCII loading score plane would be expected (Fig. 3B). In the present study, principal components were calculated for each of the 20 partitioned time windows within the stride, enabling the relative signal frequency content to be defined for different time points within the stride.

Analysis of sonomicrometry data

Changes in muscle fibre length have been shown to significantly influence myoelectric signal frequency content (Doud and Walsh, 1995). To ensure that changes in signal frequency content could be attributed to changes in motor unit recruitment patterns, mean muscle fascicle strain, taken from the sonomicrometric data, were included as covariates in the statistical analyses. They do not, however, form any further part of the work presented here. A detailed description of the analysis techniques applied to these data is therefore not included at this point, but can be found in the companion study (Hodson-Tole and Wakeling, 2008).

Statistical analysis

Significant differences in the temporal stride characteristics, mean myoelectric intensities and mean myoelectric frequencies were identified using a full-factorial general linear model ANOVA, with condition defined as a fixed factor and subject defined as a random factor in each case (SPSS® version 14.0, SPSS Inc., Chicago, IL, USA). Significant differences in the mean θ value of each locomotor condition and stride time window were assessed within each muscle using general linear model ANCOVA. Mean values were calculated from each stride and each subject. In all cases time window and condition were defined as fixed factors and mean strain included as a covariate. The inclusion of strain as a covariate ensured that significant differences in θ were not confounded by changes in muscle length, which have been shown to affect myoelectric signal frequency content (Doud and Walsh, 1995). When a significant difference was identified, *post hoc* Bonferroni tests were applied to identify the location(s) of the difference(s). The relationship between stride duration and θ was assessed using Pearson product moment

Table 2. Measured parameters of muscle architecture in each muscle studied

Muscle	Muscle mass (mg)	MTU length (mm)	Muscle length (mm)	External tendon length (mm)	Fascicle length (mm)	Pennation angle (degrees)	Volume (mm^3)	A_m (mm^2)	A_{pm} (mm^2)
Soleus	100.00±10.00	35.98±2.36	23.71±1.04	11.28±3.94	18.75±2.42	0±0	103.62±7.69	5.58±0.57	5.58±0.57
Plantaris	590.00±70.00	41.82±3.97	34.44±1.33	7.50±4.29	22.09±5.47	22±4	577.67±63.09	28.60±12.37	26.00±10.49
M. gastrocnemius	1070.00±50.00	46.32±2.02	35.06±1.61	11.33±0.83	12.23±5.50	23±6	1009.75±40.25	83.02±8.32	76.05±6.79

Values are mean ± s.d., N=6 subjects.

A_m, cross-sectional area, determined as the quotient of muscle volume and mean fascicle length; A_{pm}, physiological cross-sectional area, determined as the product of A_m and the cosine of the pennation angle.

MTU, muscle–tendon unit. * refers to tendon between the proximal end of each muscle and the insertion point of the Achilles tendon.

correlation. In all statistical analyses, results were considered to be significant when $P \leqslant 0.05$. All results are presented as mean ± s.e.m.

RESULTS

Muscle morphology

The medial gastrocnemius muscle was the largest of the three studied, having the greatest mass and longest muscle tendon unit length (Table 2). Pennation angle was very similar in the medial gastrocnemius and plantaris, although differences in muscle fascicle length were apparent (Table 2). The soleus muscle was composed of mainly parallel muscle fascicles, with no pennation angle recorded, the muscle fascicle lengths were, however, intermediate to those recorded in the plantaris and medial gastrocnemius.

Temporal stride characteristics

Mean stride temporal characteristics are shown in Fig 4 (stance and swing duration) and Fig 5 (stride frequency), with significant differences presented in Table 3. Significant differences occurred in each of the variables measured between conditions (P<0.001 all cases; Table 3). Stride duration, stance duration and swing duration all decreased with increased locomotor velocity. Increasing locomotor incline led to an increase in stride and stance duration, with a decrease in swing duration. In agreement with these findings, stride frequency increased with increased velocity and was lower during locomotion on the steepest inclines. There was no significant association between stride duration and θ in any of the muscles.

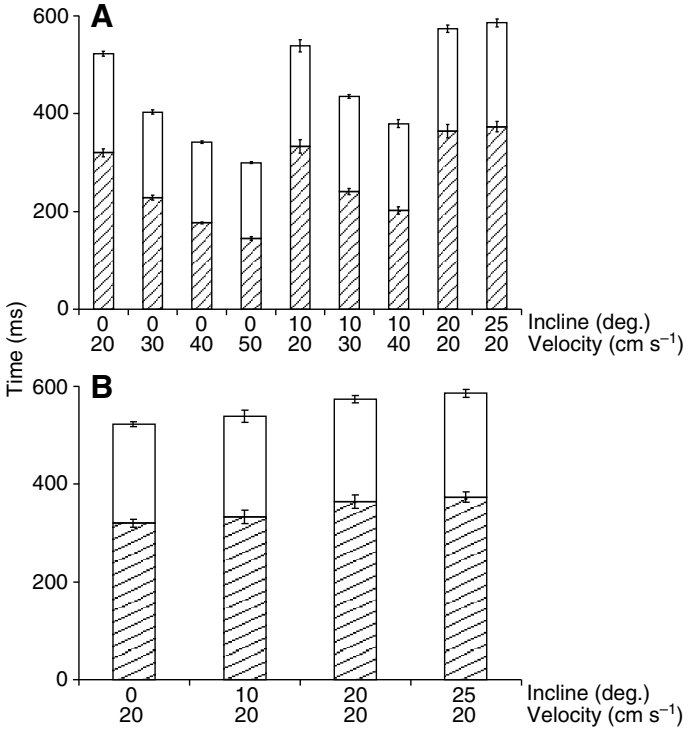

Fig. 4. (A) Temporal stride characteristics for each of the locomotor conditions and (B) incline conditions at a velocity of 20 cm s^{-1}. The whole bar represents total stride duration; the lower section (hatched) represents stance duration (mean ± s.e.m., N=12); the upper section (white) represents swing duration (mean ± s.e.m., N=12; incline in degrees; velocity in cm s^{-1}).

Characteristics of the myoelectric signals from the plantaris muscle

Within the plantaris muscle mean myoelectric intensity differed significantly between locomotor conditions (P<0.01), with greater intensities occurring at faster velocities (Fig. 6). The slower velocities (20 and 30 cm s^{-1}) on the level treadmill (0°) had significantly smaller mean myoelectric intensities than the faster velocities (0° at 40 and 50 cm s^{-1}; $P \leqslant 0.02$, all cases). Values at 0° 20 cm s^{-1} were also significantly smaller than locomotion on a 10°

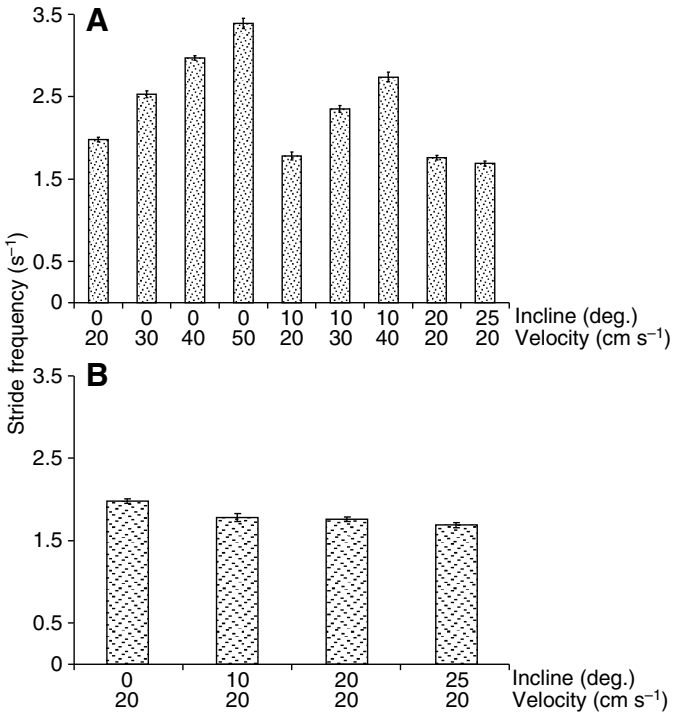

Fig. 5. Stride frequency recorded for (A) each locomotor condition and (B) all conditions at a velocity of 20 cm s^{-1} (mean ± s.e.m., N=12; incline in degrees; velocity in cm s^{-1}).

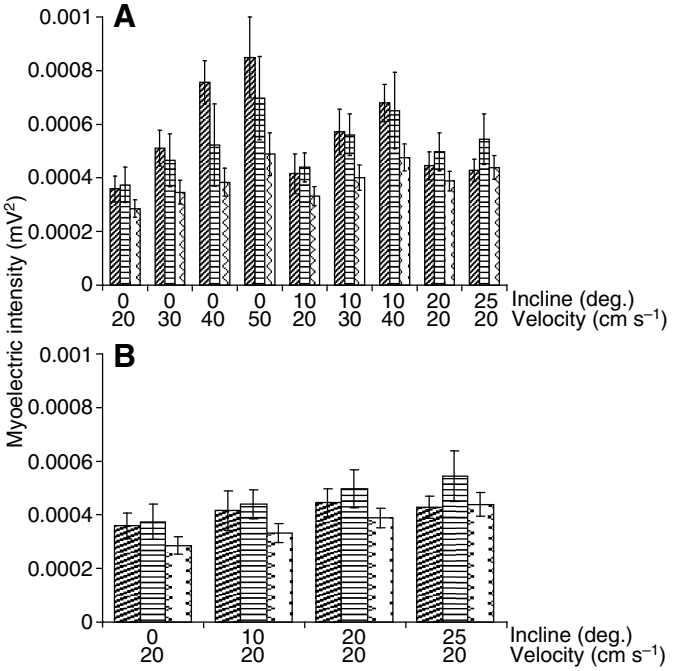

Fig. 6. Myoelectric intensities recorded from the plantaris (hatched), soleus (horizontal stripe) and medial gastrocnemius (zig-zag) in (A) each locomotor condition and (B) incline conditions at a velocity of 20 cm s^{-1} (incline in degrees; velocity in cm s^{-1}). Values are mean ± s.e.m. (N=6 for each muscle).

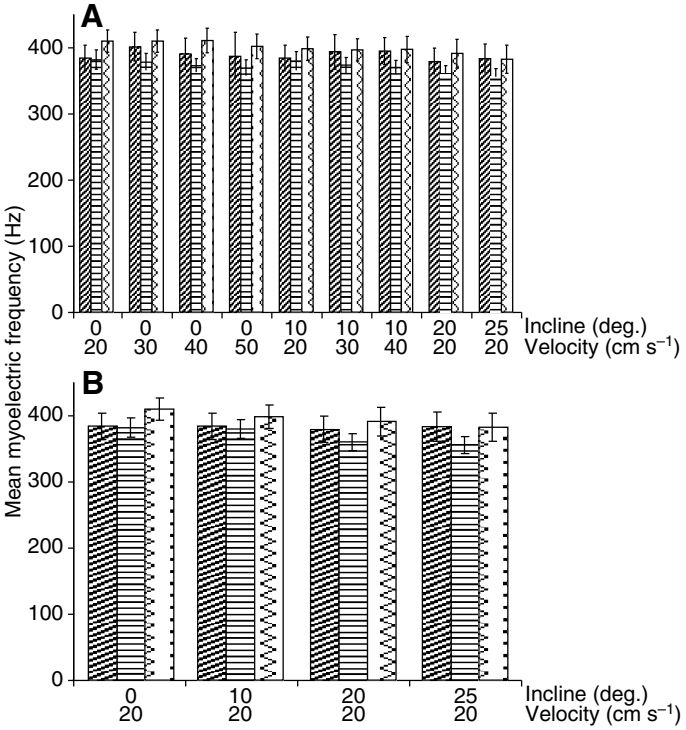

Fig. 7. Mean myoelectric frequencies recorded from the plantaris (hatched), soleus (horizontal stripe) and medial gastrocnemius (zig-zag) in (A) each locomotor condition and (B) incline conditions at a velocity of 20 cm s^{-1} (incline in degrees; velocity in cm s^{-1}). Values are mean ± s.e.m. (N=6 for each muscle).

incline at 30 and 40 cm s^{-1} ($P \leqslant 0.012$, both cases). The slowest velocity (20 cm s^{-1}) on the steepest inclines (20 and 25°) also had significantly smaller mean myoelectric intensities than locomotion at 0° at 40 and 50 cm s^{-1} ($P<0.001$, all cases) and 10° at 40 cm s^{-1} ($P \leqslant 0.02$, both cases).

Mean myoelectric frequency content for the plantaris did not differ significantly between locomotor conditions (P=0.162; Fig. 7). Mean θ values for the plantaris, under each condition, are shown in Fig. 6. In the diagram each point represents the mean PCI–PCII loading score for a time window representing 1/20 of the stride duration. In all conditions, the points resulted in a clear loop, which always followed a clockwise path, although the size and shape of the loop differed between conditions. Faster velocities were also associated with more of the points having a positive PCII loading score. There were no significant differences in θ between conditions (P=0.058). Significant differences did, however, exist between time windows, showing that θ differed significantly over the time course of the stride ($P<0.001$). These differences were, however, confounded by a significant positive association that occurred between θ and muscle fascicle strain ($P<0.001$).

Characteristics of the myoelectric signals from the soleus muscle

In the soleus muscle mean myoelectric intensity differed significantly between locomotor conditions (P=0.003; Fig. 6). There was a trend for increasing intensity with faster velocities and greater inclines. Intensities were significantly smaller at 0° 20 cm s^{-1} compared to 0° 50 cm s^{-1} and 10° 40 cm s^{-1} ($P \leqslant 0.025$, both cases). In addition intensities at 0° 50 cm s^{-1} were significantly greater than at 10° 20 cm s^{-1} (P=0.05).

Significant differences in mean myoelectric frequency were found between conditions in the soleus ($P<0.001$; Fig. 7). Values were significantly lower at 20° 20 cm s^{-1} and 25° 20 cm s^{-1} compared to 0° 20 and 30 cm s^{-1} and 10° 20 cm s^{-1} ($P \leqslant 0.045$, all cases). Mean θ values for each condition and time window are shown in Fig. 8. As in the plantaris, plotting PCI-PCII loading scores for each time window in the PCI-PCII loading score plane resulted in a distinct loop being formed for each condition. In the soleus muscle the loop was also always in a clockwise direction although it was predominantly composed of negative PCII loading scores. The size and shape of the loop changed between locomotor

Table 3. Temporal stride characteristics in each locomotor condition

Condition	Stride duration (ms)	Stance duration (ms)	Swing duration (ms)	Stride frequency (stride s^{-1})
0° 20 cm s^{-1}	522.5±10.0^{a}	320.2±8.3^{a}	202.3±4.9^{a,f}	2.0±0.0^{a}
0° 30 cm s^{-1}	403.2±7.0^{b}	228.1±4.9^{b}	175.1±4.1^{b,c,d,f}	2.5±0.0^{b}
0° 40 cm s^{-1}	342.1±2.9^{c}	176.8±2.2^{c}	165.3±2.8^{b,c,d}	3.0±0.0^{c}
0° 50 cm s^{-1}	299.8±5.1^{c}	144.4±3.9^{c}	155.4±2.2^{b,c,d}	3.4±0.1^{d}
10° 20 cm s^{-1}	539.3±20.5^{a,d}	333.2±13.8^{a,d}	206.1±12.7^{a,b,e,f}	1.8±0.0^{e}
10° 30 cm s^{-1}	434.9±7.0^{b}	241.2±6.2^{b}	193.7±3.6^{a,b,e,f}	2.4±0.0^{f}
10° 40 cm s^{-1}	379.8±14.6^{b,c}	201.8±7.6^{b,c}	178.0±8.3^{a,c,d,f}	2.7±0.1^{g}
20° 20 cm s^{-1}	574.1±16.3^{d,e}	364.5±13.9^{d,e}	209.6±7.6^{a,e,f}	1.8±0.0^{e}
25° 20 cm s^{-1}	585.8±13.8^{e}	373.2±10.6^{e}	212.6±8.5^{a,e,f}	1.7±0.0^{e}

Values are means ± s.e.m., N=12.
In each column values marked with different superscript letters differed significantly ($P \leqslant 0.05$, all cases).

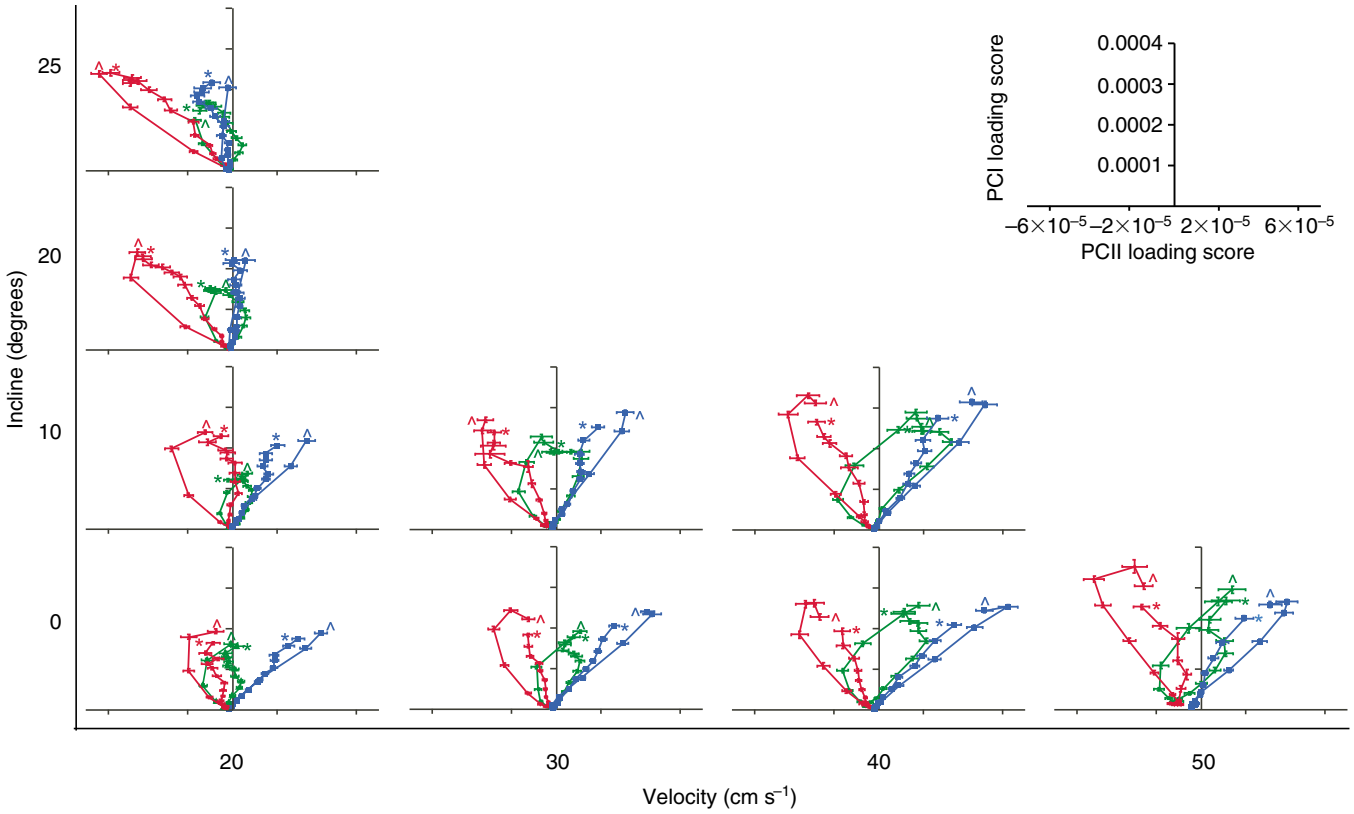

Fig. 8. Principal component loading scores for PCI and PCII from the plantaris (green), soleus (red) and medial gastrocnemius (blue) muscles during each locomotor condition. Each point shows the mean ± s.e.m. pooled from each muscle from six subjects. There are 20 points on each graph, which represent the 20 time windows within each stride. *Time points corresponding to 0% stride duration; ^time points corresponding to 100% stride duration. Points for the soleus and plantaris always track in a clockwise direction, whereas points for the medial gastrocnemius follow an anti-clockwise loop, except during the incline conditions 20° and 25° where a figure-of-eight configuration occurs. PCI loading score values are indicators of the level of muscle activity, with higher values indicating a greater level of activity. A scale bar is shown on the right.

conditions, with the loop tending to get broader in conditions with faster locomotor velocities. This trend was reflected in the results of the statistical analysis with significant differences in θ occurring between conditions ($P<0.001$) and time windows ($P<0.001$). Significant differences were identified between 0° 20 cm s^{-1} and 0° 40 and 50 cm s^{-1} ($P\leqslant0.025$, both cases). In addition, significant differences existed between 10° 20 cm s^{-1} and 0° 40 cm s^{-1} ($P<0.001$), 0° 50 cm s^{-1} ($P<0.001$) and 10° 40 cm s^{-1} ($P=0.011$). There were also significant differences in θ between time windows ($P<0.001$). The general trend was for θ during the mid-stride time windows to differ significantly to those recorded at the beginning and end of the stride. There was no significant association between θ and muscle fascicle strain ($P=0.098$), so changes in θ were not influenced by changes in muscle fascicle length.

Characteristics of the myoelectric signals from the medial gastrocnemius muscle

Significant differences in mean myoelectric intensity occurred between conditions in the medial gastrocnemius muscle ($P<0.001$; Fig. 6). Again there was a trend for greater intensities at faster velocities. Intensities at 0° 20 cm s^{-1} were significantly smaller compared with intensities at 0° 50 cm s^{-1}, 10° 30 and 40 cm s^{-1} and 25° 20 cm s^{-1} ($P\leqslant0.041$, all cases). Values at 0° 30 cm s^{-1} were also significantly smaller than those at 0° 50 cm s^{-1} and 10° 40 cm s^{-1} ($P\leqslant0.04$, both cases). In addition, there were significant differences between values recorded at 10° 20 cm s^{-1} and both 0° 50 cm s^{-1} and 10° 40 cm s^{-1} ($P\leqslant0.03$, both cases).

Significant differences in mean myoelectric frequencies were identified between conditions in the medial gastrocnemius muscle ($P<0.001$; Fig. 7). In this instance the mean frequency at 25° 20 cm s^{-1} was significantly lower than all locomotor velocities at 0° incline ($P\leqslant0.043$, all cases); in addition a significant difference also occurred between 0° 40 cm s^{-1} and 20° 20 cm s^{-1} ($P=0.035$). Mean values of θ for each condition and time window in the medial gastrocnemius muscle are shown in Fig. 6. The direction and shape of the PCI–PCII loading score loop was found to change markedly between conditions. For all conditions, except 20 cm s^{-1} at 20° and 25° inclines, the loop followed an anti-clockwise direction. During the two steepest inclines the PCI-PCII loading score loop followed a figure-of-eight pattern, with the first loop occurring in a clockwise direction and the second loop following an anti-clockwise direction. The intersection between the two loops occurred between time windows 6 and 19 at 20° 20 cm s^{-1} and between points 8 and 19 at 25° 20 cm s^{-1}. In both cases the position of time window 18 relative to time window 17 defined the direction of the second loop. There were significant differences in θ between conditions ($P<0.001$) and time windows ($P<0.001$). In addition there was a significant relationship between θ and muscle fascicle strain ($P=0.004$). The co-efficient for this relationship was, however, negative, meaning that greater values of θ were associated with lower muscle fascicle strains, so changes in θ were not confounded

by changes in muscle fascicle strain. When comparing locomotor conditions there were significant differences between values of θ recorded at 0° 50 cm s^{-1} and values recorded at 20 cm s^{-1} at 0°, 10° and 20° ($P \leqslant 0.025$). Differences in θ between time windows are shown in Fig. 7C, once again there were significant differences between values recorded in the mid-stride time windows and early and late stride times.

DISCUSSION

In agreement with the stated experimental hypotheses it was found that myoelectric intensity increased with increasing locomotor velocity in each of the three muscles investigated. Myoelectric intensity also increased in response to increased locomotor incline, this was, however, only identified in the medial gastrocnemius and soleus muscles. Changes in locomotor velocity and incline therefore resulted in different responses of the three muscles, indicating that these factors may have placed different demands on each. The hypotheses that changes in the myoelectric signal frequency component, quantified by θ, would occur in response to changes in locomotor velocity and incline were also supported by results from soleus and medial gastrocnemius muscles. We have interpreted this as reflecting changes in motor unit recruitment patterns, the details of which are discussed below.

Patterns of motor unit recruitment in the ankle extensor muscles

Relative signal frequency components were represented by PCI–PCII loading, with negative PCII loading score values indicating a greater relative low frequency component, whereas positive PCII loading score values indicated a greater relative high frequency component. In agreement with previous work (Hodson-Tole and Wakeling, 2007; Wakeling and Rozitis, 2004), PCI loading scores were a close correlate to myoelectric intensity (r^2=0.99). Values of θ were determined from vector plots in the PCI–PCII loading score plane, with higher values associated with relatively more low frequency signal component and lower values associated with relatively more high frequency component. Differences in θ, caused by differences in PCII loading scores, where PCI loading scores were similar, represented fundamental differences in the relative frequency component of the myoelectric signal and therefore corresponded to differential motor unit recruitment (Wakeling and Rozitis, 2004). In each of the three motor unit populations studied the vector plot of the θ values resulted in distinct loops in each of the muscles, demonstrating that differential recruitment of motor units occurred (Figs 6, 7). In all cases the largest θ values were recorded in the soleus muscle, reflecting the predominantly slow population of motor units within this muscle. The smallest θ values were recorded in the medial gastrocnemius muscle, reflecting the predominantly fast population of motor units. The plantaris muscle had the greatest mix of motor unit types and it is within this muscle that the greatest variation in θ across the time course of a stride was recorded. The gross differences in motor unit populations between the muscles studied (Armstrong and Phelps, 1984), were therefore evident in the results presented.

Within each muscle distinct patterns of changes in myoelectric frequency content across the time course of a stride were apparent in all conditions (Figs 6, 7). In the soleus and plantaris muscles the myoelectric activity was initially characterised by relatively more low frequency content, represented by the larger θ values. The later stages of myoelectric activity were characterised by more relative high frequency content, represented by the smaller θ values. In these muscles it is therefore likely that slower motor units were recruited at the onset of myoelectric activity, with faster motor units recruited later in the myoelectric burst. By contrast, myoelectric frequency content in the medial gastrocnemius muscle indicated a reversal of this pattern (Fig. 8). In this muscle myoelectric activity was initially characterised by smaller θ values and hence relatively greater high frequency content. Later in the burst of activity relatively more low frequency content was recorded, represented by greater θ values. In this muscle it therefore seems likely that faster motor units were recruited at the onset of myoelectric activity, with subsequent recruitment of slower motor units. Preferential recruitment of faster motor units was therefore apparent in the medial gastrocnemius during most of the locomotor conditions. The reason for such a recruitment strategy within this muscle is unclear. The medial gastrocnemius muscle was the largest of the three muscles studied (Table 2) and has been reported to have distinct proximal and distal compartments (De Ruiter et al., 1995). In the present study, data were collected from the proximal region, which has been described as having a predominantly fast, type IIB, fibre population (Armstrong and Phelps, 1984). The innervations and physiological characteristics of these compartments have been shown to differ (De Ruiter et al., 1995; De Ruiter et al., 1996). It is likely that a coordinated strategy of activation and motor unit recruitment within each compartment occurs to facilitate controlled force production, and is an area of study that warrants further investigation. The data presented here, are likely to represent only one compartment and therefore do not represent the recruitment strategy within the whole muscle. The results do, however, highlight that preferential recruitment of faster motor units can and does occur within a population of different motor unit types. Surprisingly, there was no significant difference in the θ values recorded between conditions in the plantaris muscle. This may reflect the range of motor unit types present leading to the changes in motor unit recruitment patterns not being as distinct as those seen in motor unit populations dominated by a single motor unit type.

The experimental data support the hypothesis that locomotion on an incline would lead to a significant increase in low frequency myoelectric signal component, as this was found to occur in all of the muscles studied (Fig. 8). The most dramatic change was seen in the medial gastrocnemius muscle where, at the steepest inclines (25°), the greatest θ values for the muscle were recorded. Similar trends were also apparent in the soleus and plantaris muscles. In addition to the greater θ values recorded in the medial gastrocnemius the direction and shape of the PCI–PCII loading score loop changed. The figure-of-eight pattern recorded began with a loop following a clockwise path, indicating that relatively more low frequency content occurred at the onset of myoelectric activity than at the end. This reflected preferential recruitment of slower motor units at this time and meant that during the two steepest conditions (20° and 25°) all muscles studied demonstrated orderly recruitment of motor units from the slowest through to the fastest. Some factor or combination of factors relating to locomotion on an inclined treadmill therefore favours the preferential recruitment of slower motor units in the rat ankle extensor muscles.

The change in the relative myoelectric frequency component, and hence motor unit recruitment patterns, seen in the medial gastrocnemius and the differences in the myoelectric signals between the motor unit populations studied suggests that the musculoskeletal system employs a number of motor unit recruitment patterns and strategies to facilitate smooth, co-ordinated movement. Whether the changes and/or differences between muscles are driven by muscle fascicle length changes, differences in muscle fascicle strain rates, activation–deactivation kinetics of the recruited motor units and/or

some form of neural drive is as yet unknown and warrants further investigation. Potential motor unit recruitment strategies will be discussed below in light of the results presented here.

Motor unit recruitment predicted by the size principle

The size principle predicts that motor unit recruitment should occur in an orderly fashion from the slowest through to the fastest motor units (Henneman et al., 1965a; Henneman et al., 1965b). In addition, deactivation of motor units should occur in the reverse order, from the fastest units through to the slowest. The functional advantages of recruiting slower motor units first can be broken into two main categories. Firstly, slower motor units are more fatigue resistant and can provide sufficient force for a wide number of activities such as maintenance of posture and walking. Faster motor units fatigue more rapidly and so would not be able to sustain force production over a prolonged period of time. Secondly, orderly recruitment of motor units is proposed to facilitate smooth force increment (Henneman and Olson, 1965; Henneman et al., 1965b). Myoelectric activity in both the soleus and plantaris muscles was initially characterised by greater relative low frequency content, followed by a relative increase in the high frequency component. It can therefore be interpreted, in accordance with the predictions of the size principle, that motor units were recruited in an orderly fashion from the slowest through to the fastest. If the predictions of the size principle were to hold true, however, plotting θ in the PCI–PCII loading score plane would lead to a single line representing activation and deactivation within the muscle with no difference in the PCI–PCII loading scores from either phase. This would result from the fact that the size principle predicts that a given level of muscle activity (represented by PCI loading scores) is achieved by activation of one combination of motor units (represented by θ). When such a recruitment pattern is simulated using a volume conductor model and the resulting myoelectric signals, assessed activation and deactivation follow the same path on the PCI-PCII loading score vector graph (Fig. 3A) (Wakeling, 2008). PCI-PCII loading score vector plots for the muscles studied were, however, found to form distinct, looping patterns (Fig. 8). This means that, for the motor unit populations studied, a given level of muscle activity was achieved with more than one combination of active motor units, contravening the predictions of the size principle. The soleus and plantaris did, however, recruit slower motor units first, indicating that the suggested functional advantages of recruiting slower motor units prior to faster ones may hold true in these muscles.

Motor unit recruitment related to activation–deactivation kinetics

It has previously been identified that activation–deactivation properties play an important role in determining the ability of a muscle to produce mechanical work and hence power during different locomotor tasks (Caiozzo and Baldwin, 1997; Johnston, 1991). This factor can be influential for two reasons. Firstly, activation times are longer in slow motor units (Burke et al., 1973) meaning that they need longer to produce a given level of force. Activating slower motor units first may therefore be a strategy to ensure that these motor units are able to produce the required force at a specific time and in conjunction with faster motor units, which are able to produce force more rapidly. Slower motor units also have longer deactivation times (Burke et al., 1973), so it might be expected that these units would be deactivated earlier than faster motor units to ensure that force production reached a minimum in all motor units simultaneously. Illustrating such a recruitment strategy using the PCI–PCII loading score vector plots would result in a circular plot, following a clockwise path (Fig. 3B). This would represent relatively more low frequency content at the onset of myoelectric activity, representing activity in slow motor units, with the composition of the signal subsequently including relatively more high frequency components as more faster motor units were recruited and slower motor units deactivated. This pattern closely matches that seen in the soleus and plantaris muscles, but not the medial gastrocnemius (Fig. 8). The assessment of such a relationship is hampered, however, by the complicated changes in activation–deactivation kinetics, which occur as a result of changes in strain (Brown et al., 1999; Close, 1972; Josephson and Stokes, 1999), motor unit firing frequency (Roszek et al., 1994) and muscle fascicle strain rates (Brown and Loeb, 2000).

Activation–deactivation kinetics may also have influenced motor unit recruitment patterns as the result of a recruitment strategy to maximise metabolic efficiency. Studies on human single fibres have shown that, based on myosin isoforms, slower muscle fibres have a lower metabolic cost during both isometric and shortening contractions (He et al., 2000). Recruiting slower motor units may therefore provide a metabolically cheap mechanism that drives motor unit recruitment. The significantly longer stride durations that occurred during the incline conditions (Fig. 4, Table 3) may have enabled adequate force production from the slower motor units, despite their longer activation–deactivation times, leading to a cheaper metabolic cost than would have been incurred by recruiting faster motor units. Particular note should be made of the medial gastrocnemius muscle here, as PCI–PCII loading score vector plots during the longest stride durations, and steepest inclines, were distinctly different to those seen in other conditions (Fig. 8). This represents a clear change in motor unit recruitment strategy. For such a recruitment strategy to exist a significant positive relationship between θ and stride duration would be expected. The results, however, indicate that such a relationship did not exist.

A mechanical basis for motor unit recruitment

The longer stride durations seen in the incline conditions may also favour preferential recruitment of slower motor units based on their force–velocity properties. It is predicted that isotonic mechanical power output is maximised at approximately 0.3 V_{max} (maximum unloaded shortening velocity) (Hill, 1938). This has led to the prediction that, during normal locomotion, power generating muscles should operate at shortening velocities corresponding to those that produce maximum power during isovelocity contractions (Hill, 1950; Lutz and Rome, 1996). Such a relationship has been identified in a number of studies including those of swimming fish (Rome et al., 1992; Rome et al., 1988) and jumping frogs (Lutz and Rome, 1996). The longer stride durations that occurred during incline locomotion would mean that force production could occur at lower strain rates, which would favour mechanically efficient power production in the slower motor units (Rome et al., 1988). As the speed of contraction increases, greater power output occurs in faster motor units. If mechanical power output were a determining factor of motor unit recruitment patterns it might be expected that there would be a positive relationship between the recruitment of faster motor units and muscle fascicle shortening velocities. Such a relationship has been reported to occur in the medial gastrocnemius of humans during cycling (Wakeling et al., 2006). How widespread such a phenomenon is, has yet to be determined. This topic therefore warrants further investigation and forms the basis of the investigation presented in the companion paper (Hodson-Tole and Wakeling, 2008).

Conclusion

The results presented here indicate that myoelectric signal frequency content from the three ankle extensor muscles of the rat change significantly in response to changes in locomotor velocity and incline. These changes have been interpreted to represent changes in patterns of motor unit recruitment. The patterns of motor unit recruitment presented do not match the predictions of the size principle if it is strictly adhered to. Both the soleus and plantaris muscles followed an orderly pattern of motor unit recruitment from slower to faster motor units in all conditions. By contrast, the medial gastrocnemius demonstrated preferential recruitment of faster motor units in all conditions except those on an incline >20°. The changes in motor unit recruitment patterns that occurred between and within muscles indicate the flexibility that exists in motor unit recruitment strategies. It is proposed that, in addition to the size principle, motor unit recruitment may be influenced by the intrinsic properties of each muscle, namely activation–deactivation kinetics and force–velocity properties.

Michael Boyd and John Thurlborne are gratefully acknowledged for their assistance with surgical procedures and care of the animals, and also Georgina Disney who helped collect muscle architectural measurements. Karin Jespers and Pattama Ritruechai kindly helped with the data collection process. The use of the sonomicrometry equipment was by kind permission of Prof. Alan Wilson.

REFERENCES

Albuquerque, E. X. and Thesleff, S. (1968). A comparative study of membrane properties of innervated and chronically denervated fast and slow skeletal muscles of the rat. *Acta Physiol. Scand.* **73**, 471-480.

Armstrong, R. B. and Phelps, R. O. (1984). Muscle fiber type composition of the rat hindlimb. *Am. J. Anat.* **171**, 259-272.

Bawa, P., Binder, M. D., Ruenzel, P. and Henneman, E. (1984). Recruitment order of motoneurons in stretch reflexes is highly correlated with their axonal conduction velocity. *J. Neurophysiol.* **52**, 410-420.

Brody, L. R., Pollock, M. T., Roy, S. H., De Luca, C. J. and Celli, B. (1991). pH-induced effects on median frequency and conduction velocity of the myoelectric signal. *J. Appl. Physiol.* **71**, 1878-1885.

Brown, I. E. and Loeb, G. E. (2000). Measured and modeled properties of mammalian skeletal muscle. IV. Dynamics of activation and deactivation. *J. Muscle Res. Cell Motil.* **21**, 33-47.

Brown, I. E., Cheng, E. J. and Loeb, G. E. (1999). Measured and modeled properties of mammalian skeletal muscle. II. The effects of stimulus frequency on force-length and force-velocity relationships. *J. Muscle Res. Cell Motil.* **20**, 627-643.

Burke, R. E., Levine, D. N., Tsairis, P. and Zajac, F. E., 3rd (1973). Physiological types and histochemical profiles in motor units of the cat gastrocnemius. *J. Physiol.* **234**, 723-748.

Caiozzo, V. J. and Baldwin, K. M. (1997). Determinants of work produced by skeletal muscle: potential limitations of activation and relaxation. *Am. J. Physiol.* **273**, C1049-C1056.

Close, R. (1964). Dynamic properties of fast and slow skeletal muscles of the rat during development. *J. Physiol.* **173**, 74-95.

Close, R. I. (1972). The relations between sarcomere length and characteristics of isometric twitch contractions of frog sartorius muscle. *J. Physiol.* **220**, 745-762.

Close, R. and Luff, A. R. (1974). Dynamic properties of inferior rectus muscle of the rat. *J. Physiol.* **236**, 259-270.

De Ruiter, C. J., de Haan, A. and Sargeant, A. J. (1995). Physiological characteristics of two extreme muscle compartments in the medial gastrocnemius muscle of the rat. *Acta Physiol. Scand.* **153**, 313-324.

De Ruiter, C. J., Habets, P. E., de Haan, A. and Sargeant, A. J. (1996). *In vivo* IIX and IIB fiber recruitment in gastrocnemius muscle of the rat is compartment related. *J. Appl. Physiol.* **81**, 933-942.

Doud, J. R. and Walsh, J. M. (1995). Muscle fatigue and muscle length interaction: effect on the EMG frequency components. *Electromyogr. Clin. Neurophysiol.* **35**, 331-339.

Gillis, G. B. and Biewener, A. A. (2001). Hindlimb muscle function in relation to speed and gait: *in vivo* patterns of strain and activation in a hip and knee extensor of the rat (*Rattus norvegicus*). *J. Exp. Biol.* **204**, 2717-2731.

He, Z.-H., Bottinelli, R., Pellegrino, M. A., Ferenczi, M. A. and Reggiani, C. (2000). ATP consumption and efficiency of human single muscle fibers with different myosin isoform composition. *Biophys. J.* **79**, 945-961.

Henneman, E. and Olson, C. B. (1965). Relations between structure and function in the design of skeletal muscles. *J. Neurophysiol.* **28**, 581-598.

Henneman, E., Somjen, G. and Carpenter, D. O. (1965a). Excitability and inhibitability of motoneurons of different sizes. *J. Neurophysiol.* **28**, 599-620.

Henneman, E., Somjen, G. and Carpenter, D. O. (1965b). Functional significance of cell size in spinal motoneurons. *J. Neurophysiol.* **28**, 560-580.

Hill, A. V. (1938). The heat of shortening and the dynamic constants of muscle. *Proc. R. Soc. Lond. B Biol. Sci.* **126**, 136-195.

Hill, A. V. (1950). The dimensions of animals and their muscular dynamics. *Sci. Prog.* **38**, 209-230.

Hodson-Tole, E. F. and Wakeling, J. M. (2007). Variations in motor unit recruitment patterns occur within and between muscles in the running rat (*Rattus norvegicus*). *J. Exp. Biol.* **210**, 2333-2345.

Hodson-Tole, E. F. and Wakeling, J. M. (2008). Motor unit recruitment paterns 2: the influence of myoelectric intensity and muscle fascicle strain rate. *J. Exp. Biol.* **211**, 1893-1902.

Johnston, I. A. (1991). Muscle action during locomotion: a comparative perspective. *J. Exp. Biol.* **160**, 167-185.

Josephson, R. and Stokes, D. (1999). Work-dependent deactivation of a crustacean muscle. *J. Exp. Biol.* **202**, 2551-2565.

Kupa, E. J., Roy, S. H., Kandarian, S. C. and De Luca, C. J. (1995). Effects of muscle fiber type and size on EMG median frequency and conduction velocity. *J. Appl. Physiol.* **79**, 23-32.

Luff, A. R. and Atwood, H. L. (1972). Membrane properties and contraction of single muscle fibers in the mouse. *Am. J. Physiol.* **222**, 1435-1440.

Lutz, G. J. and Rome, L. C. (1996). Muscle function during jumping in frogs. II. Mechanical properties of muscle: implications for system design. *Am. J. Physiol.* **271**, C571-C578.

McPhedran, A. M., Wuerker, R. B. and Henneman, E. (1965a). Properties of motor units in a heterogeneous pale muscle (M. gastrocnemius) of the cat. *J. Neurophysiol.* **28**, 85-99.

McPhedran, A. M., Wuerker, R. B. and Henneman, E. (1965b). Properties of motor units in a homogeneous red muscle (soleus) of the cat. *J. Neurophysiol.* **28**, 71-84.

Mendez, J. and Keys, A. (1960). Density and composition of mammalian muscle. *Metabolism* **9**, 184-188.

Mundermann, A., Wakeling, J. M., Nigg, B. M., Humble, R. N. and Stefanyshyn, D. J. (2006). Foot orthoses affect frequency components of muscle activity in the lower extremity. *Gait Posture* **23**, 295-302.

Peter, J. B., Barnard, R. J., Edgerton, V. R., Gillespie, C. A. and Stempel, K. E. (1972). Metabolic profiles of three fiber types of skeletal muscle in guinea pigs and rabbits. *Biochemistry* **11**, 2627-2633.

Powell, P. L., Roy, R. R., Kanim, P., Bello, M. A. and Edgerton, V. R. (1984). Predictability of skeletal muscle tension from architectural determinations in guinea pig hindlimbs. *J. Appl. Physiol.* **57**, 1715-1721.

Rome, L., Sosnicki, A. and Choi, I. (1992). The influence of temperature on muscle function in the fast swimming scup. II. The mechanics of red muscle. *J. Exp. Biol.* **163**, 281-295.

Rome, L. C., Funke, R. P., Alexander, R. M., Lutz, G. J., Aldridge, H., Scott, F. and Freadman, M. (1988). Why animals have different muscle fibre types. *Nature* **335**, 824-827.

Roszek, B., Baan, G. C. and Huijing, P. A. (1994). Decreasing stimulation frequency-dependent length-force characteristics of rat muscle. *J. Appl. Physiol.* **77**, 2115-2124.

Schiaffino, S. and Reggiani, C. (1996). Molecular diversity of myofibrillar proteins: gene regulation and functional significance. *Physiol. Rev.* **76**, 371-423.

Schiaffino, S., Gorza, L., Sartore, S., Saggin, L., Ausoni, S., Vianello, M., Gundersen, K. and Lomo, T. (1989). Three myosin heavy chain isoforms in type 2 skeletal muscle fibres. *J. Muscle Res. Cell Motil.* **10**, 197-205.

Sherrington, C. (1929). Ferrier Lecture: some functional problems attaching to convergence. *Proc. R. Soc. Lond. B Biol. Sci.* **105**, 332-362.

von Tscharner, V. (2000). Intensity analysis in time-frequency space of surface myoelectric signals by wavelets of specified resolution. *J. Electromyogr. Kinesiol.* **10**, 433-445.

von Tscharner, V. (2002). Time-frequency and principal-component methods for the analysis of EMGs recorded during a mildly fatiguing exercise on a cycle ergometer. *J. Electromyogr. Kinesiol.* **12**, 479-492.

von Tscharner, V. and Goepfert, B. (2006). Estimation of the interplay between groups of fast and slow muscle fibers of the tibialis anterior and gastrocnemius muscle while running. *J. Electromyogr. Kinesiol.* **16**, 188-197.

Wakeling, J. M. (2004). Motor units are recruited in a task-dependent fashion during locomotion. *J. Exp. Biol.* **207**, 3883-3890.

Wakeling, J. M. (2008). Patterns of motor recruitment can be determined using surface EMG. *J. Electromyogr. Kinesiol.* doi:10.1016/j.elekin.2007.09.006.

Wakeling, J. M. and Rozitis, A. I. (2004). Spectral properties of myoelectric signals from different motor units in the leg extensor muscles. *J. Exp. Biol.* **207**, 2519-2528.

Wakeling, J. M. and Syme, D. A. (2002). Wave properties of action potentials from fast and slow motor units of rats. *Muscle Nerve* **26**, 659-668.

Wakeling, J. M., Pascual, S. A., Nigg, B. M. and Von Tscharner, V. (2001a). Surface EMG shows distinct populations of muscle activity when measured during sustained sub-maximal exercise. *Eur. J. Appl. Physiol.* **86**, 40-47.

Wakeling, J. M., Von Tscharner, V., Nigg, B. M. and Stergiou, P. (2001b). Muscle activity in the leg is tuned in response to ground reaction forces. *J. Appl. Physiol.* **91**, 1307-1317.

Wakeling, J. M., Kaya, M., Temple, G. K., Johnston, I. A. and Herzog, W. (2002). Determining patterns of motor recruitment during locomotion. *J. Exp. Biol.* **205**, 359-369.

Wakeling, J. M., Uehli, K. and Rozitis, A. I. (2006). Muscle fibre recruitment can respond to the mechanics of the muscle contraction. *J. R. Soc. Interface* **3**, 533-544.